

Fluctuation of Gaps in Hadronization at Phase Transition

Rudolph C. Hwa¹ and Qing-hui Zhang²

¹Institute of Theoretical Science and Department of Physics
University of Oregon, Eugene, OR 97403-5203, USA

²Department of Physics, McGill University, Montreal, Quebec H3A 2T8, Canada

Abstract

Event-by-event fluctuations of hadronic patterns in heavy-ion collisions are studied in search for signatures of quark-hadron phase transition. Attention is focused on a narrow strip in the azimuthal angle with small Δy . The fluctuations in the gaps between particles are quantified by simple measures. A scaling exponent α is shown to exist around T_c . An index ξ is shown to characterize the critical fluctuation; it is a numerical constant $\xi = 0.05 \pm 0.01$. All the measures considered in this gap analysis are experimentally observable. Whether or not the theoretical predictions, based on simulations using 2-dimensional Ising model, are realistic for heavy-ion collisions, analysis of the experimental data suggested here should be carried out, since the existence of a scaling behavior is of interest in its own right.

1 Introduction

If a quark-gluon system created in a heavy-ion collision at high energy undergoes a second-order phase transition to hadrons, one should expect large fluctuations in the hadron densities from region to region. Thus in any small interval of hadronization time the particles produced on the surface of the system, where the temperature T is at the critical temperature T_c , should form patterns of clusters and voids of all sizes. The question is how such fluctuations can be detected. Since the detector integrates over the hadronization time, the hadron patterns formed at different times, when added, tend toward a uniform sum. In Refs. [1, 2] we have studied the problem and found a way to overcome the difficulty. On the one hand, one must make severe cuts in the transverse momentum p_T (accepting particles only in a narrow window of width Δp_T), while on the other hand, appropriate measures that are insensitive to the randomization process following hadronization should be used to quantify the critical fluctuations. We proposed a void analysis that identifies the scaling properties of the fluctuations. The suggested measures in the analysis are in the two-dimensional space of rapidity (y) and azimuthal angle (ϕ). The analysis has been applied to the NA49 data of Pb - Pb collisions at CERN-SPS [3], but remains to be considered for the data collected at BNL-RHIC.

In this paper we aim at simplifying the experimental problem of detecting the critical fluctuation, while making one of the theoretical parameters in the void analysis more experimentally relevant. They are accomplished by reducing the 2D space to 1D so that a void becomes a gap. The study of gaps in rapidity was undertaken by us earlier in connection with multiparticle production in hadronic collisions [4]. The proposed gap analysis has been applied to the NA22 data [5] and provides a way of testing the predictions of the dynamical models on soft processes. We now apply the gap analysis to the phase transition problem in heavy-ion collisions. Besides showing what can be expected theoretically, we believe that the suggestions made here are more amenable to the experimental situation. An important outcome of this study is the identification of a numerical constant that characterizes the critical fluctuation. It can be checked by experiment.

Our theoretical tool, as in [1, 2], is still the simulation of critical phenomenon on the 2D Ising lattice. Not only is the simulation simple to execute, it is also physically relevant, since the quark-hadron phase transition is very likely to be in the same universality class as the Ising system [6]. We map the 2D Ising lattice to the surface of the quark-gluon plasma cylinder formed in a central collisions of heavy ions. We select a row in the lattice and map that to a strip on the plasma cylinder confined to a narrow interval in rapidity. Our proposed analysis is for the experimental examination of the fluctuation of gaps between particles in the azimuthal ϕ variable.

2 Gap Analysis on the Lattice and for the Experiments

The relationship between the Ising problem and the hadron density problem has been discussed in detail in Refs. [1, 2]. We summarize here only the essentials for what is needed in this paper.

We start with a 2D lattice of size L^2 , where $L = 288$. On the lattice we define cells of

size ϵ^2 , where $\epsilon = 4$. The density ρ_i at the i th cell is defined to be

$$\rho_i = \lambda c_i^2 \theta(c_i) \quad , \quad (1)$$

where c_i is the net spin at cell i defined to be positive along the overall magnetization, i.e.,

$$c_i = \text{sgn} \left(\sum_{j \in L^2} \sigma_j \right) \sum_{j \in i} \sigma_j, \quad (2)$$

σ_j being the lattice spin at site j , and λ an unspecified factor relating c_i^2 to the particle density in y - ϕ space. Near T_c , ρ_i fluctuates from cell to cell; however, the existence of correlation of all length scales leads to clusters of all sizes formed out of neighboring cells having non-vanishing ρ_i .

In Refs. [1, 2] we considered bins of size δ^2 , with δ being integral multiples of ϵ . We regarded a bin to be empty if the average bin density, $\bar{\rho}_b$, is less than a threshold density ρ_0 . We then defined a void to be a collection of contiguous empty bins, connected by at least one side between neighboring empty bins. The measure used to quantify the fluctuation of void sizes was shown to be insensitive to the value of ρ_0 .

Without undercutting the importance of doing the void analysis on experimental data with high statistics, especially at high energies, we want now to consider in this paper the possibility of doing a similar analysis in 1D, since if clustering of hadrons occurs in 2D, they should also be visible in 1D. Not only will the statistics improve, there will also be no need to do binning to define voids, as we shall see.

Let us consider a row of C cells, where we initially take $C = L/\epsilon = 72$. We map that row to a slice of the plasma cylinder in the central region with width Δy in rapidity. What Δy is will be discussed below. We also will limit p_T to a narrow interval Δp_T , as discussed extensively in Refs. [1, 2]. Thus we have only the azimuthal angle ϕ as our space of variable. The row of C cells is mapped to the interval $0 \leq \phi < 2\pi$.

We simulate N_e configurations (where $N_e = 3 \times 10^5$) on the Ising lattice in 2D at $T = T_c$, and determine the density ρ_i at each cell in each configuration. The simulation cannot be done in 1D because a 1D Ising system does not exhibit critical behavior. From a 2D configuration we choose an arbitrary row and examine the values of ρ_i in each cell with $1 \leq i \leq C$. The value of λ in Eq. (1) is effectively set to 1 in what we do with ρ_i , since we always compare it to a threshold ρ_0 in units of λ . We define an occupied cell to be one in which

$$\rho_i > \rho_0 \quad , \quad (3)$$

and we place one (and only one) particle at cell i . If $\rho_i \leq \rho_0$, then it is an empty cell. In mapping to the ϕ variable, we place a particle at ϕ_i randomly in the interval $(i-1)2\pi/C \leq \phi < i2\pi/C$, when the i th cell satisfies Eq. (3). Thus after the whole row is mapped to the ϕ variable, there are N particles in the ϕ space, where N fluctuates from event to event. An event corresponds to a configuration on the lattice.

On the lattice the average number of occupied cells $\langle N \rangle$ in a row, after averaging over all configurations, depends on the threshold ρ_0 . In the experiment the average number of particles $\langle N \rangle$ in the ϕ space depends on $\Delta y \Delta p_T$. In our analysis we shall vary ρ_0 . The

predicted dependence of our measure on ρ_0 is to be checked by experiment by varying $\Delta y \Delta p_T$. In that sense the variable ρ_0 is not a theoretical parameter devoid of experimental relevance.

In an experiment of heavy-ion collisions the single-particle inclusive distribution in ϕ , $dn/d\phi$, may not be uniform, because the impact parameter is not always exactly zero (even if a centrality cut is made), or because the detector efficiency is not symmetric in ϕ , mostly likely both. It is then better to use the cumulative variable X [7, 8], defined in our case by

$$X(\phi) = \int_0^\phi \frac{dn}{d\phi'} d\phi' \bigg/ \int_0^{2\pi} \frac{dn}{d\phi'} d\phi' . \quad (4)$$

The range $0 \leq \phi \leq 2\pi$ is thus mapped to $0 \leq X \leq 1$, and the density of particles in X , dn/dX , is uniform. The distribution $dn/d\phi$ is determined after many events, but the variable X is used for exclusive distributions event-by-event. In a simulation $dn/d\phi$ is uniform, if N_e is large; we nevertheless use the X variable between 0 and 1 just so that our proposed gap analysis corresponds to what is to be done with experimental data.

Consider an event with N particles in our window, labeled by $i = 1, \dots, N$, located in the X space at X_i , ordered in accordance to $X_i < X_{i+1}$. Now define the distance between neighboring particles by

$$x_i = X_{i+1} - X_i, \quad i = 0, \dots, N, \quad (5)$$

with $X_0 = 0$ and $X_{N+1} = 1$ being the boundaries of the X space. We call these x_i 's gaps, which clearly satisfy

$$\sum_{i=0}^N x_i = 1. \quad (6)$$

Let us define for each event the moments

$$G_q = \frac{1}{N+1} \sum_{i=0}^N x_i^q, \quad (7)$$

which, for positive q , puts more emphasis on the large gaps than the small ones. The set $\{G_q\}$ with $2 \leq q \leq Q$, Q being some number less than 10, say, will be our quantification of the event structure. The set fluctuates from event to event, especially at the critical point. Our method is to use $\{G_q\}$ as a basis to construct a measure that can reveal the critical behavior.

Among the various erraticity measures considered in Ref. [4] we choose S_q for our consideration here, since it has the simplest behavior. Starting with the definition

$$s_q = \langle G_q \ln G_q \rangle, \quad (8)$$

where the average $\langle \dots \rangle$ is performed over all events, S_q is defined by

$$S_q = s_q / s_q^{st} \quad (9)$$

where s_q^{st} is as defined in Eq. (8) but with the statistical contribution to G_q only. Thus the deviation of S_q from 1 is a measure of how strong the dynamical fluctuations are relative

to the statistical fluctuations. In our simulation we generate N random numbers between 0 and 1 to populate the X space for the calculation of G_q^{st} . In an experiment one can do something similar to generate a random event.

We shall study the dependence of S_q on q for various values of ρ_0 , using configurations simulated on the Ising lattice. The same can be done with the experimental data from heavy-ion collisions. If hadrons are formed in the latter due to a second-order phase transition, then the experimental S_q should reveal some features that are similar to our theoretical S_q to be presented below.

3 Results on Critical Fluctuations

Using $N_e = 3 \times 10^5$ configurations simulated on the Ising lattice at $T = T_c = 2.315$ in units of J/k_B [1], where J is the near neighbor coupling and k_B the Boltzmann constant, we have determined S_q for a range of ρ_0 . For $\rho_0 = 20$ the dependence of S_q on q is shown in a log-log plot in Fig. 1. The solid line is a straight-line fit of the calculated result, giving strong evidence for the power-law behavior

$$S_q \propto q^\alpha. \quad (10)$$

The value of the exponent is $\alpha = 1.67 \pm 0.02$. The fact that $\ln S_q$ deviates unambiguously from 0 implies that S_q is a statistically significant measure of nontrivial dynamical fluctuation. The power-law behavior is not necessarily a consequence of the dynamics of critical phenomenon, since similar behavior has been found before in the case of hadronic collisions [4]. However, the exponent α is indicative of critical fluctuations; it is an order of magnitude larger than the value of $\alpha = 0.156$ obtained for pp collisions at $\sqrt{s} = 20$ GeV.

To have one exponent α for all q is a very economical description of the critical fluctuations. We can then investigate the dependence of α on ρ_0 . Before so doing, let us first find a replacement of ρ_0 by some quantity that is directly measurable. In the preceding section we have related ρ_0 to the intervals $\Delta y \Delta p_T$ as the variable under experimental control that can be used to tune the average multiplicity $\langle N \rangle$ accepted in the ϕ window. Thus $\langle N \rangle$ is a quantity that is both experimentally observable and theoretically computable on the lattice. It is therefore a suitable replacement for ρ_0 . Nevertheless, we prefer to use an even better one that is the average number of gaps $\langle M \rangle$, which is also observable. On the lattice in accordance to our convention of counting gaps in Eqs. (5) and (6), we have simply $M = N + 1$. However, it should be recalled that in our simulation we have adopted the rule that, when ρ_i exceeds ρ_0 , only one particle is placed in a cell, not more, no matter how high ρ_i is. That procedure makes sense in view of our measure G_q of the event structure, since a tightly packed cell with many particles in it would have very small gaps that make negligible contribution in Eq. (7). Experimentally, if there are particles whose momenta are indistinguishable, or nearly so, whether they are separately counted or not also makes no significant difference in the calculation of G_q . Thus to allow for such possibilities it is better to count the number of distinguishable gaps, rather than the number of particles.

On the lattice we have simulated the configurations for a range of ρ_0 from 20 to 200. For every value of ρ_0 we can calculate the average number of gaps, $\langle M \rangle$. Figure 2 shows the dependence of $\langle M \rangle$ on ρ_0 at T_c . The straight-line segments are just the linear interpolations

between neighboring points of ρ_0 where the calculation has been made. With such a definitive relationship at hand, any quantity that depends on ρ_0 will in the following be shown as a function of $\langle M \rangle$, so as to render it amenable to experimental verification.

For each of the higher values of ρ_0 examined, we have found power-law behavior of S_q , as in Fig. 1. Thus the exponent α can be determined in each case. In Fig. 3 we show the dependence of α on $\langle M \rangle$. Remarkably, the dependence is very linear. If we parameterize it as

$$\alpha = \alpha_0 + \xi \langle M \rangle, \quad (11)$$

we obtain

$$\alpha_0 = -0.258, \quad \xi = 0.055. \quad (12)$$

The nature of critical fluctuation is now seen to be reduced to a simple formula, Eq. (11), when the moments of gaps are used to describe the event structure. If we further put emphasis on the property that is independent of $\langle M \rangle$, then the slope ξ in Eq. (12) emerges as a numerical output of the theory that relies on no numerical input. This is perhaps the most succinct characterization of the critical phenomenon, beside the critical exponents. The latter depend on the temperature of a critical system near T_c . In heavy-ion collisions T is not directly observable, so the corresponding critical exponents cannot be measured experimentally (see, however, Ref. [9]). Here we have an index ξ that is eminently measurable and is the only numerical constant that can be meaningfully associated with critical fluctuation.

So far our study has been done only at $T = T_c$. To see how the results change when T deviates from T_c , we repeat the above analysis for a range of T . Figure 4 shows S_q vs q in log-log plot for $2.27 < T < 2.80$ in units of J/k_B . Note that linearity is quickly lost when T goes below $T_c = 2.315$. For $T > T_c$ the linearity persists for a limited range $2.315 < T < 3.1$, but the slope is reduced. For $T > 3.2$ the dependence bends over at high q and the linearity is lost. For the range of T where α can be determined from linear fits, we show in Fig. 5 $\alpha(T)$ up to $T = 2.8$. The sharp peak that occurs at $T = T_c$ is a remarkable manifestation of the critical behavior. For T less than T_c , so many hadrons are produced that the gap distribution rapidly tends toward the statistical. For T larger than T_c , fewer hadrons are produced, and it takes more $T - T_c$ difference for the statistical fluctuation to dominate. If T were experimentally controllable, the measurement of $\alpha(T)$ would be an excellent way to determine the critical temperature of the quark-gluon system. That being not the case in reality, we can only learn from Figs. 4 and 5 that, if the system hadronizes in a range of T around T_c , the most significant portion of the contribution to S_q would come from the immediate neighborhood of $T = T_c$, and that only the α value around T_c is experimentally relevant.

The above analysis is done for $\rho_0 = 20$. We can, of course, repeat the analysis for other values of ρ_0 . In each case we find the peak value of α at T_c . At each T where α can be meaningfully determined, we can investigate its dependence on $\langle M \rangle$, just as we have done in Fig. 3 at T_c . In each case a linearity is found that allows us to determine the slope index ξ in Eq. (11). The result is shown in Fig. 6, where $\xi(T)$ also exhibits a peak at T_c . We can now conclude that if hadronization is to occur around T_c , we expect the measurable value of ξ to be around 0.05.

Having established the properties of the observables as functions of T due to the dynamics of the critical system, we now investigate the question of stability with respect to changes in the size of the detector window, which is kinematical. We have so far considered a lattice of size 72×72 cells, from which we choose one row of $C = 72$ cells from each configuration. We now want to vary the length and width of the row. We shall do so by setting T at T_c . First, we consider a row of $C = 54$ cells from each configuration, and later a row of $C = 36$ cells. In each case it does not matter whether the row is mapped to a correspondingly shorter range in ϕ , since $dn/d\phi$ is converted to dn/dX in the X space before the gap analysis is performed. However, the average number of gaps $\langle M \rangle$ does change, so the simulation with shorter rows does correspond to a shorter ranges of ϕ in the experiment. In Fig. 7 we show the result on α vs. $\langle M \rangle$ for the $C = 72, 54$, and 36 cells. The straight lines are linear fits, which are evidently very good. The values of the slope ξ are :

$$\begin{aligned} \xi &= 0.055 \pm 0.005, & C &= 72 \\ &0.057 \pm 0.005, & C &= 54 \\ &0.048 \pm 0.007, & C &= 36 \end{aligned} \tag{13}$$

The case of $C = 36$ cells yields a slightly lower value and relatively larger errors, as is reasonable, since there are fewer points in a shorter range. Nevertheless, all three values of ξ agree within errors. We therefore conclude that ξ is stable against variations in the length of the ϕ window.

Next, we consider variations in the width of the ϕ window. In our simulation so far we have used only rows with 1-cell width. In an experiment the width Δy of a window in ϕ will have to be adjusted in order to vary $\langle M \rangle$. To check the stability of our result against variations in the width of our strip on the Ising lattice, we consider combinations of two and three rows. Let k be the row index, and i the cell index in the row, as before. Thus the location of a cell on the lattice is now denoted by ki . We take r adjacent rows and combine them by performing vertical average of r cells at each horizontal position i , i. e., we define

$$\rho_i = \frac{1}{r} \sum_{k=1}^r \rho_{ki} \tag{14}$$

and then proceed in the gap analysis using ρ_i as in the preceding section. It is important that the r rows be adjacent so that the short-range vertical correlation of the cells can influence the value of ρ_i so as to reflect its dynamical content; otherwise, if the r rows are randomly chosen, the averaging in Eq. (14) tend to render ρ_i more statistical and its distribution in i more uniform. In short, taking r adjacent rows corresponds to widening Δy in the experiment. In our calculation we consider only the case $r = 2$ and 3 . Note that we take the average in Eq. (14) and then vary ρ_0 to change $\langle M \rangle$. We could have added ρ_{ki} (without dividing by r) and not vary ρ_0 ; that is equivalent to averaging ρ_{ki} and dividing ρ_0 by r . Our chosen procedure allows more continuous change in ρ_0 .

The result of our analysis for $r = 1, 2$ and 3 , and $C = 72$, are shown in Fig. 8. Roughly speaking, the slopes are essentially the same within errors, so ξ may be regarded as independent of r . More precisely, we find

$$\xi = 0.055 \pm 0.005, \quad r = 1,$$

$$\begin{aligned}\xi &= 0.044 \pm 0.003, & r &= 2, \\ \xi &= 0.045 \pm 0.003, & r &= 3.\end{aligned}\tag{15}$$

The slight decrease in ξ , as r increases, is not unreasonable, since averaging over r rows tends to suppress dynamical fluctuations. In the limit r becoming very large, clearly only statistical fluctuations remain. We may summarize Eqs. (13), (15) and Fig. 6 by the grand average

$$\xi = 0.05 \pm 0.01.\tag{16}$$

If this can be verified by experiments, then one should be able to claim that a signature of critical transition has been observed. If the value of ξ is not confirmed, yet the power-law behavior of Eq. (10) is shown to exist in the data, with or without the linear dependence of α on $\langle M \rangle$ in Eq. (11), that would still be an exciting experimental finding, suggestive of dynamical fluctuations.

There is the usual question about final-state interaction and the dilution of the dynamical signature due to randomization. The answer depends on the type of measure for that signature. The issue has been addressed in Ref. [9], where the dependence on the number of steps of final-state scatterings is examined, in Ref. [1] where configuration mixing is considered, and in Ref. [2] where different options in simulating time evolution are investigated. What one learns from all those studies is that the measures considered are not strongly affected by the final-state randomization. Since the gap analysis is a derivative of the void analysis [1, 2], the same conclusion follows here. The one reminder that we should emphasize is that the window Δp_T in the transverse momentum should be kept as small as possible to minimize the overlap of particles emitted at different times.

4 Conclusion

We have studied the problem of even-to-event fluctuations of the hadronic patterns in phase space in heavy-ion collisions in search for detectable signatures of second-order quark-hadron phase transition. We have reduced the complication of voids in two dimensions to the simpler problem of gaps in one dimension. Using the moments of gaps to construct an entropy-like measure S_q , we have found a power-law dependence on q with an exponent α . It is the dependence of α on the average number of gaps that yields the index ξ , which serves to characterize critical fluctuation. We have found the stability of $\xi = 0.05 \pm 0.01$ against variations in the length and width of the detector window in ϕ . When the temperature of the system is moved away from T_c , the power-law behavior of S_q on q persists in a narrow range of T around T_c , and the values of α and ξ show strong peaks at T_c . Thus ξ is a measure of the critical behavior and is a number that arises out of the study of fluctuations without any numerical input. It is highly significant that ξ can be checked by experiments, since all measures leading to its determination are designed to be observable.

In heavy-ion experiments it is not difficult to make cuts in Δp_T and Δy to limit the average number of particles in a narrow strip in ϕ to the range from 10 to 40. If those particles are found to be non-uniformly distributed for every event, the gap analysis proposed here is a way to quantify those fluctuations. When the exponent α and the index ξ are found

to exist, there are numerous variables under the control of the experiments to vary. We can mention, for example, the position of the y slice, the value of p_T , the centrality of collisions, the nuclei sizes and the c.m. energy. It would be very interesting to see the dependence of ξ on the total transverse energy E_T , since it can provide us with some idea of when the critical behavior is lost as the nuclei overlap gets to be too small to create a quark-gluon plasma. Also, for nonzero impact parameter, even if critical fluctuations exist, the index ξ may depend on which sector of the ϕ space the analysis is performed, since there is no ϕ invariance in elliptic flow. One can envision a rich variety of phenomenological studies once the exponent α and index ξ are found in the experimental data. They can provide valuable information about the quark-gluon system. The application of the gap analysis to the data is therefore strongly urged.

Acknowledgment

This work was supported, in part, by the U. S. Department of Energy under Grant No. DE-FG03-96ER40972, and the Natural Science and Engineering Research Council of Canada and the Fonds FCAR of the Quebec Government.

References

- [1] R. C. Hwa, and Q. H. Zhang, Phys. Rev. C **62**, 054902 (2000).
- [2] R. C. Hwa, and Q. H. Zhang, Phys. Rev. C **64**, 054904 (2001).
- [3] C. B. Yang, preliminary report (private communication).
- [4] R. C. Hwa, and Q. H. Zhang, Phys. Rev. D **62**, 014003 (2000).
- [5] NA22 Collaboration, H. B. Liao, (private communication)
- [6] S. Gavin, A. Gocksch, and R. D. Pisarski, Phys. Rev. D **49**, 3079 (1994).
- [7] A. Białas and M. Gardzicki, Phys. Lett. B **252**, 483 (1990).
- [8] W. Ochs, Z. Phys. C **50**, 339 (1991).
- [9] R. C. Hwa and Y. F. Wu, Phys. Rev. C **60**, 054904 (1999).

Figure Captions

- Fig. 1** S_q vs q in log-log plot for $T = T_c$ and $\rho_0 = 20$.
- Fig. 2** The average number of gaps $\langle M \rangle$ vs ρ_0 at T_c .
- Fig. 3** The exponent α vs $\langle M \rangle$ at T_c .
- Fig. 4** S_q vs q in log-log plot for a range of T at $\rho_0 = 20$.
- Fig. 5** α vs T at $\rho_0 = 20$.
- Fig. 6** ξ vs T at $\rho_0 = 20$.
- Fig. 7** α vs $\langle M \rangle$ at T_c for various number of cells in a row.
- Fig. 8** α vs $\langle M \rangle$ at T_c after averaging over various number of rows.

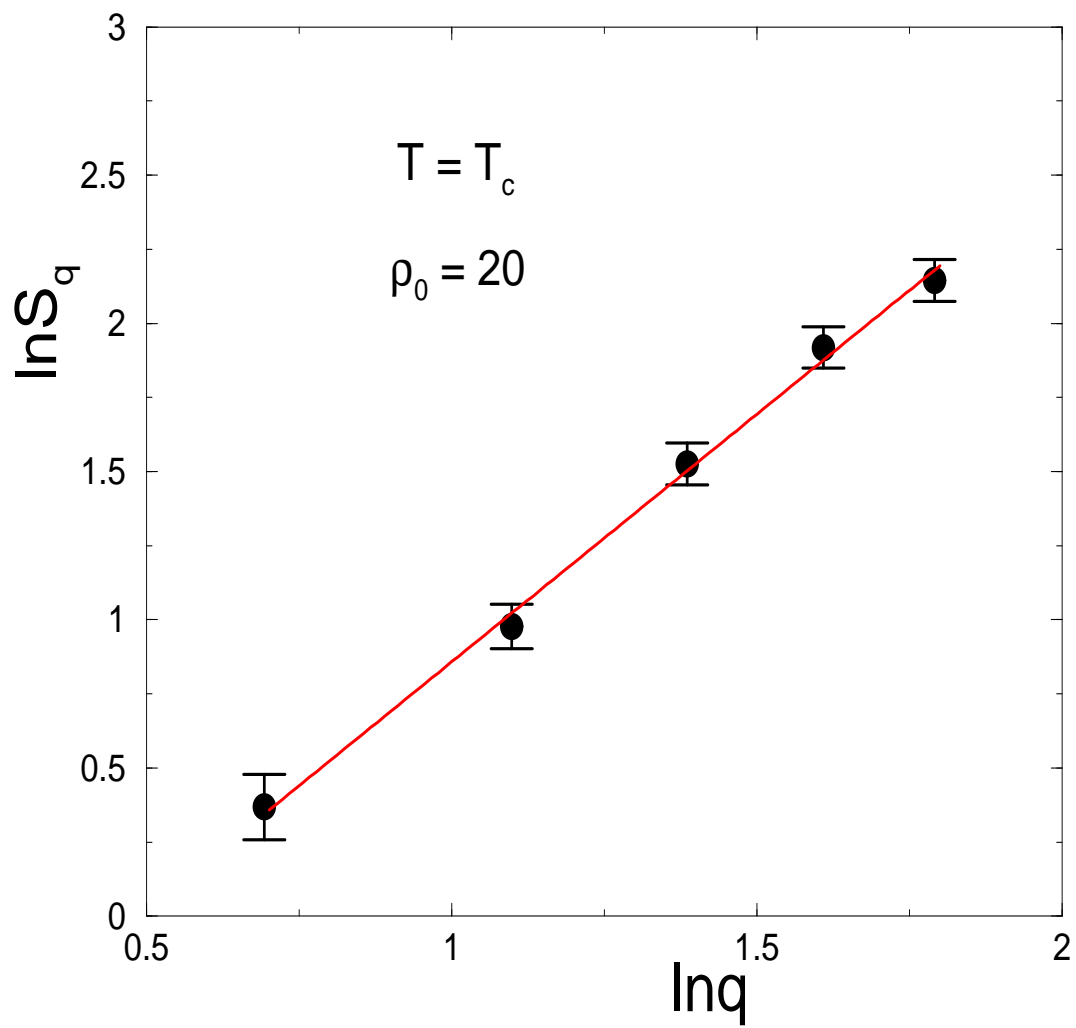


Fig.1

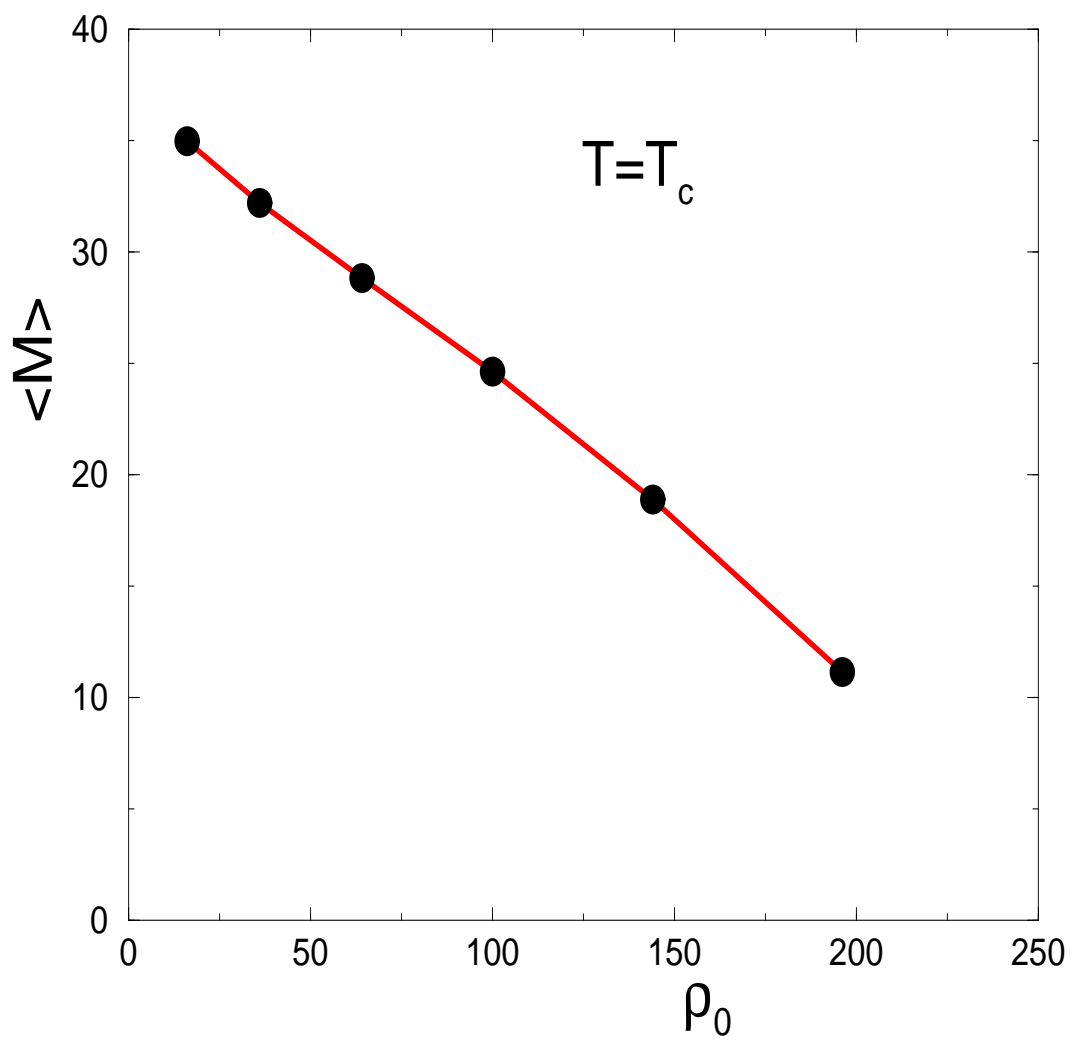


Fig.2

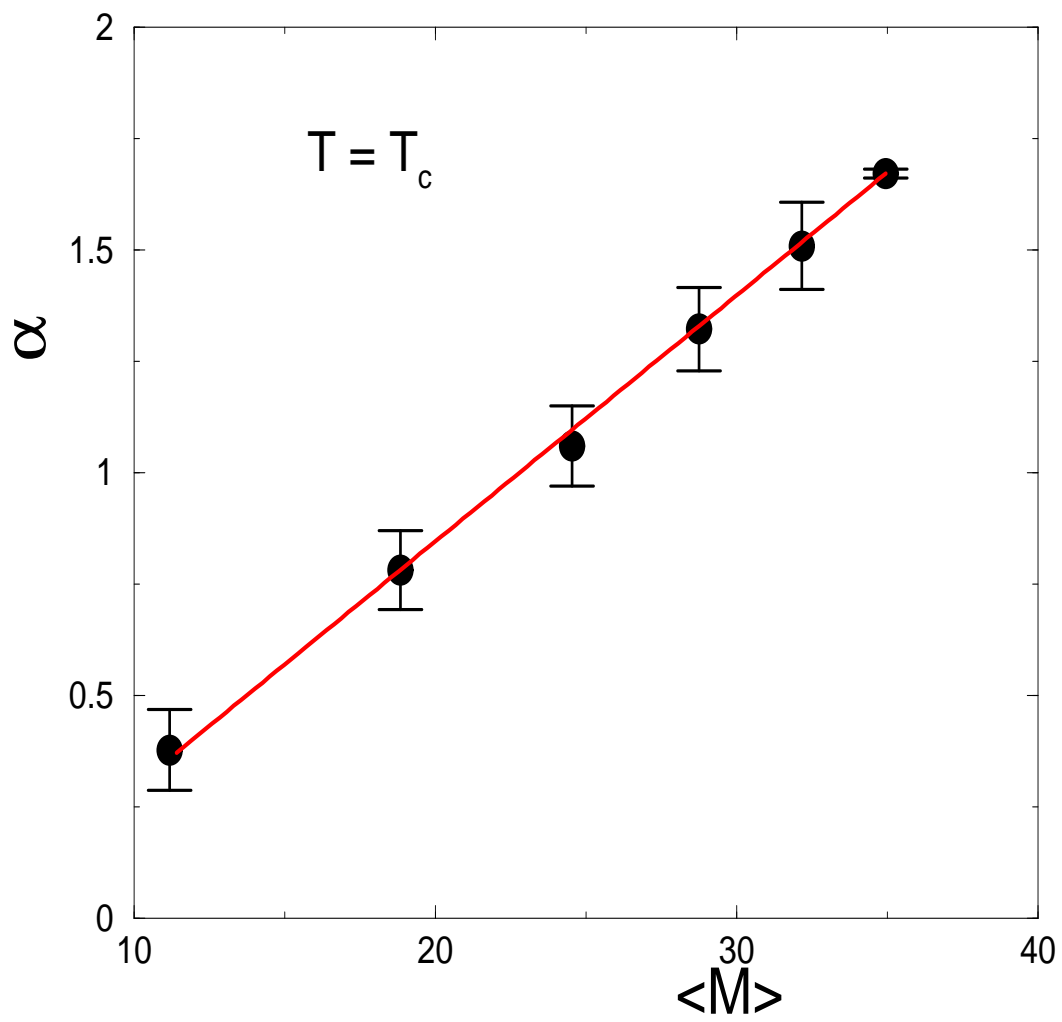


Fig.3

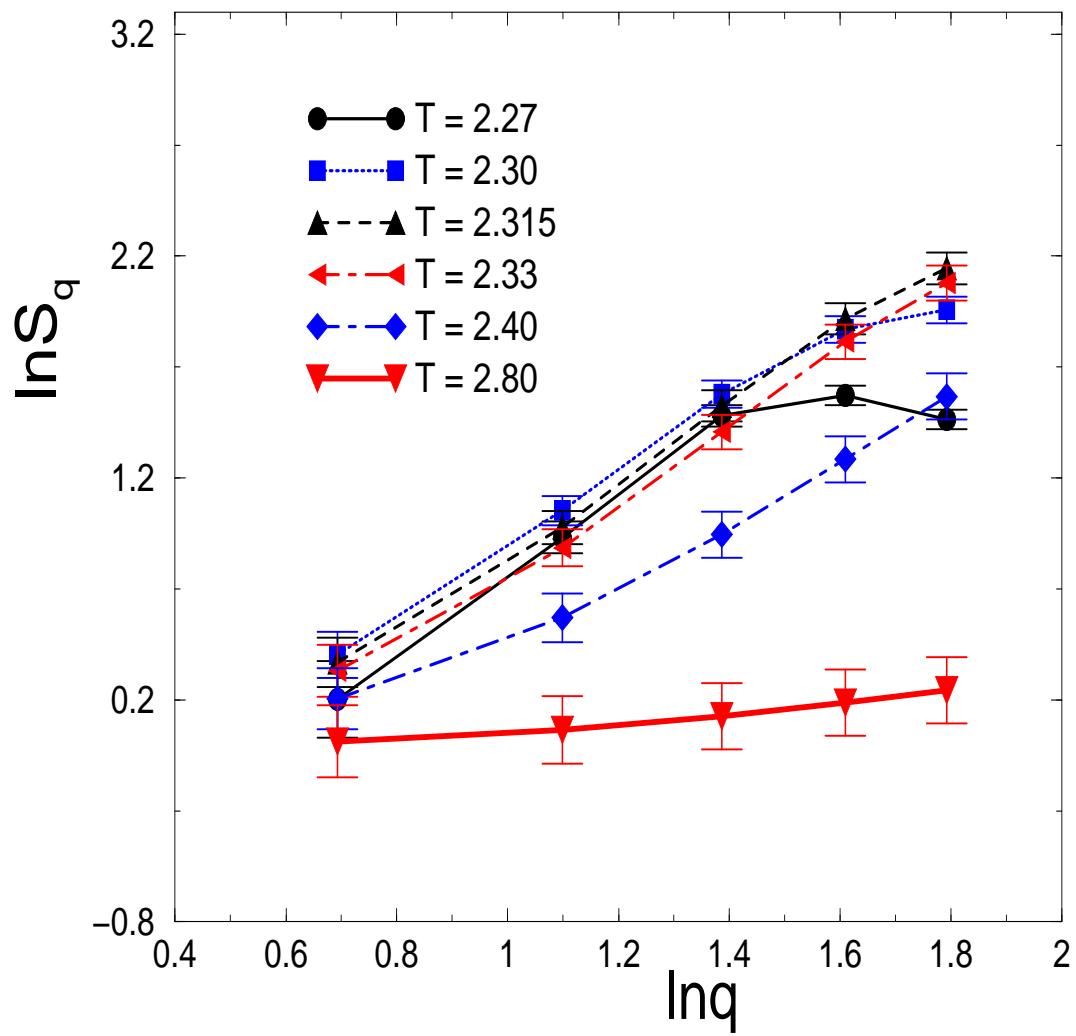


Fig.4

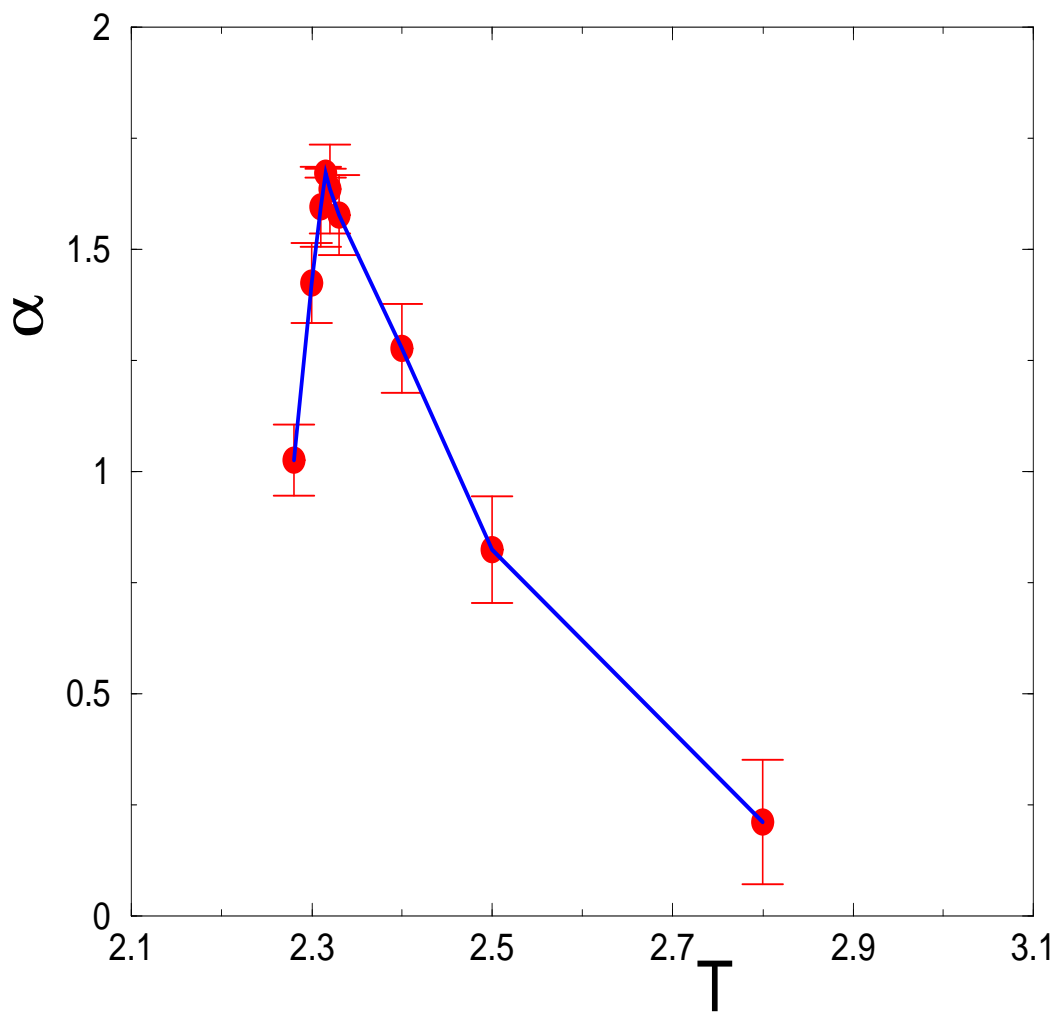


Fig.5

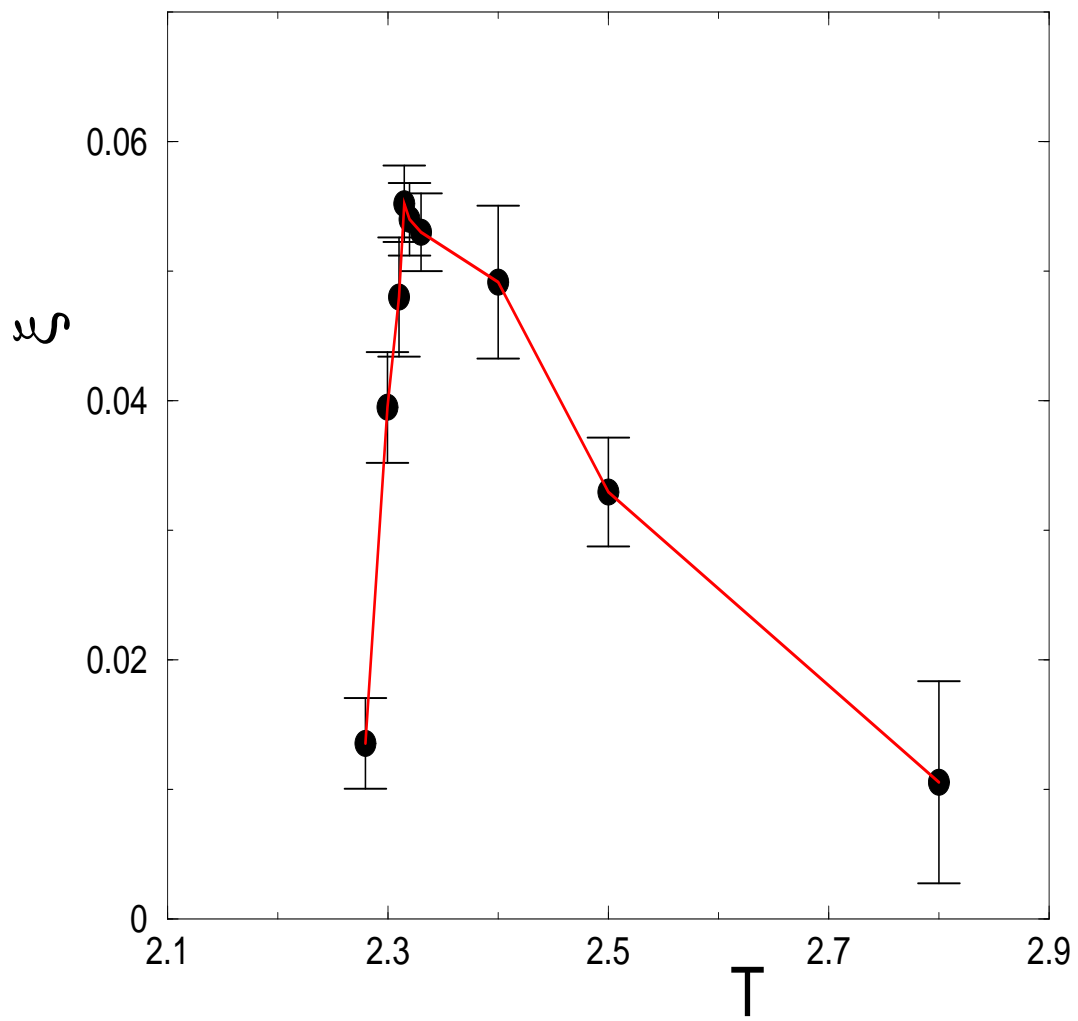


Fig.6

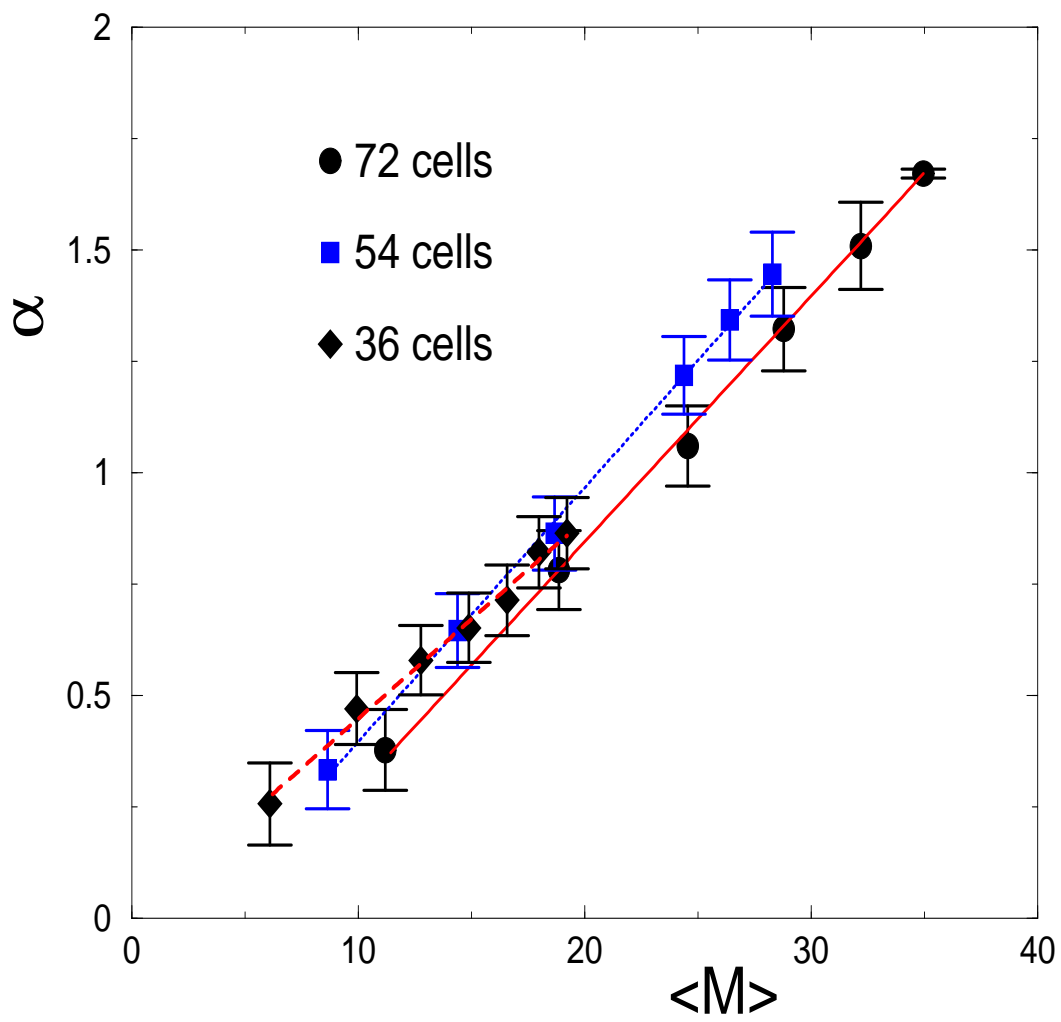


Fig.7

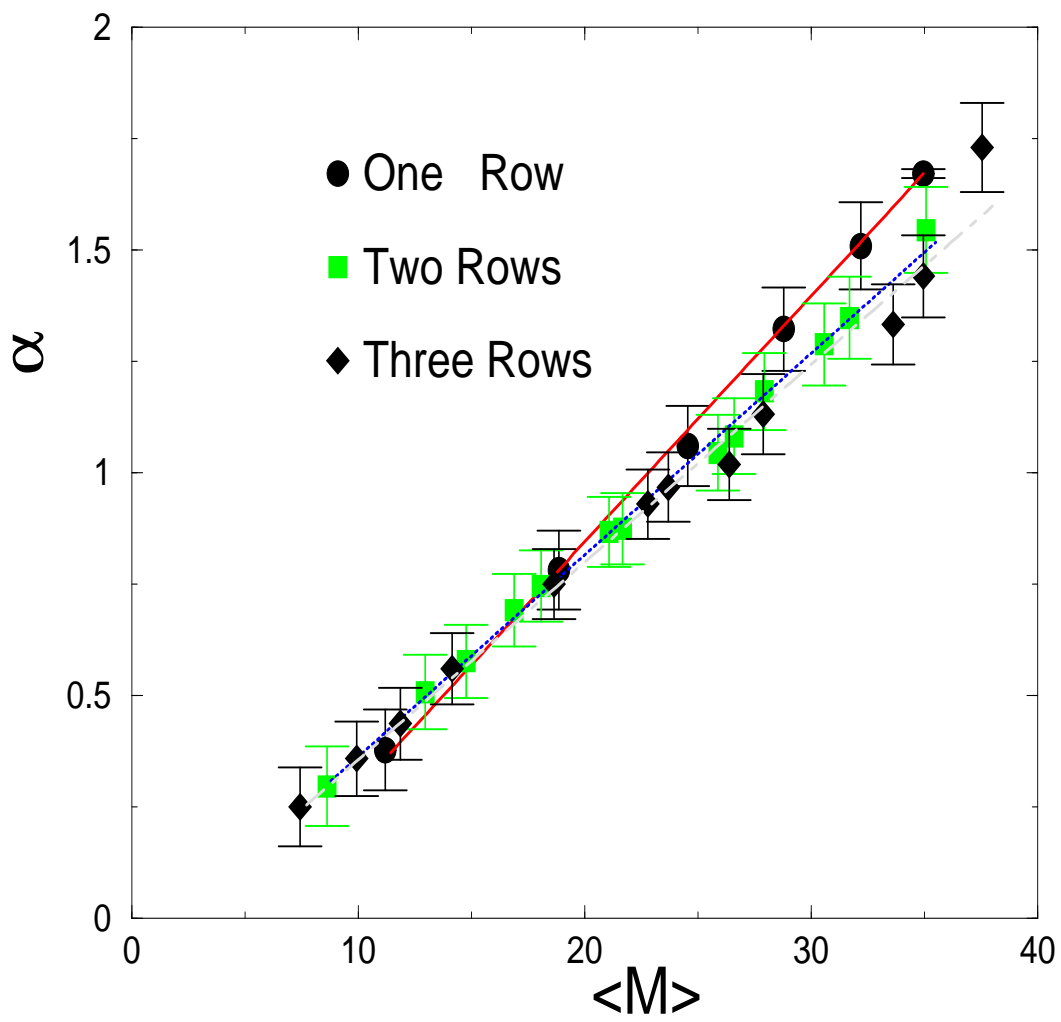


Fig.8